Contribution from the Lehrstuhl für Anorganische Chemie I, Ruhr-Universität, D-4630 Bochum, FRG, and Lehrstuhl für Allgemeine Anorganische und Analytische Chemie der Universität Gesamthochschule, D-4790 Paderborn, FRG

Acid-Catalyzed Anti → Syn Isomerization of the $\{W^V_2O_4\}^{2+}$ Core. Crystal Structures of *anti*-$[L_2W_2O_4]I_2$ and *syn*-$[L_2W_2O_4]_2(S_2O_6)I_2 \cdot 2H_2O$ (L = 1,4,7-Triazacyclononane)

Peter Schreiber,[1a] Karl Wieghardt,*[1a] Ulrich Flörke,[1b] and Hans-Jürgen Haupt[1b]

Received December 9, 1987

Preparations of yellow *syn*-$[L_2W_2O_4]I_2$ and its purple anti isomer (L = 1,4,7-triazacyclononane, $C_6H_{15}N_3$) have been achieved by air oxidation of zinc dust reduced aqueous solutions containing LWO_3 or $[L_2W_2O_5](Br_3)_2$. In acidic solution the syn isomer prevails whereas in neutral solution the anti isomer is the kinetically controlled generated product. The kinetics of the acid-catalyzed anti → syn isomerization of the $\{W_2O_4\}^{2+}$ core have been measured. Single crystals of *syn*-$[L_2W_2O_4]_2(S_2O_6)I_2 \cdot 2H_2O$ have been obtained. It crystallizes in the orthorhombic space group *Pnnm* (No. 58) with a = 12.974 (2) Å, b = 22.370 (5) Å, c = 8.612 (2) Å, V = 2499.5 (6) Å^3, and Z = 2. For the *syn*-$\{W_2O_4\}^{2+}$ core the following averaged bond distances have been determined: W=O$_t$ = 1.72 (2) Å, W—O$_b$ = 1.93 (1) Å, W—W = 2.565 (1) Å. The W_2O_2 four-membered ring is puckered. *anti*-$[L_2W_2O_4]I_2$ crystallizes in the monoclinic space group $P2_1/c$ with a = 6.838 (2) Å, b = 11.539 (3) Å, c = 14.716 (4) Å, β = 90.57 (2)°, V = 1161.3 (5) Å^3, and Z = 2. For the *anti*-$\{W_2O_4\}^{2+}$ core the bond distances are W=O$_t$ = 1.73 (1) Å, W—O$_b$ = 1.98 (1) Å, and W—W = 2.568 (1) Å. The four-membered ring is planar.

Introduction

Relatively few examples of dinuclear tungsten(V) complexes containing the bis(μ-oxo)bis(oxotungsten(V)) core, $\{W_2O_4\}^{2+}$, have been synthesized and characterized by X-ray crystallography to date.[2] The *syn*-$\{W_2O_4\}^{2+}$ unit has been identified in $[W_2O_4(edta)]^{2-}$,[3] $[W_2O_4(C_2O_4)_{2.5}]^{3-}$,[4] and $[W_2O_4F_6]^{4-}$[4] whereas the corresponding *anti*-$\{W_2O_4\}^{2+}$ core has not been structurally characterized previously.[5]

In contrast, the $\{Mo_2O_4\}^{2+}$ unit is well-known in the chemistry of molybdenum(V),[6] and both the anti and syn isomers have been characterized as diamagnetic complexes of the type $[L_2Mo_2O_4]^{2+}$ where L represents a cyclic triamine such as 1,4,7-triazacyclononane[7] or 1,5,9-triazacyclododecane.[8] It has been shown that in solution *anti*-$[L_2Mo_2O_4]^{2+}$ is irreversibly transformed by acid or base catalysis into the thermodynamically slightly more stable syn isomer.[8,15]

The preparation of the analogous tungsten(V) complexes with the 1,4,7-triazacyclononane ligand has been reported,[9] although no structural characterization had been carried out because suitable single crystals for an X-ray analysis were not available at that time. Here we wish to report the crystal structure of *anti*-$[L_2W_2O_4]I_2$ and *syn*-$[L_2W_2O_4]_2(S_2O_6)I_2 \cdot 2H_2O$. The anti isomer is converted to the syn form by acid catalysis, and the kinetics of this reaction have been measured.

Experimental Section

Preparation of *syn*-$[L_2W_2O_4]I_2$. $LWO_3 \cdot 2H_2O$[10] (0.3 g; 0.8 mmol) (L = 1,4,7-triazacyclononane) was dissolved in 0.2 M aqueous trifluoromethanesulfonic acid (15 mL) under an argon atmosphere at room temperature. Zinc dust (0.7 g) was added with stirring for 1 h, after which time a clear green solution was obtained. Exposure of this solution to air caused a color change to yellow-orange. Addition of sodium iodide (2.5 g) initiated the precipitation of yellow microcrystals, which were filtered off, washed with ethanol and ether, and air-dried; yield 0.4 g.

Anal. Calcd for $[(C_6H_{15}N_3)_2W_2O_4]I_2$: C, 15.27; H, 3.20; N, 8.90; I, 26.89; W, 38.95. Found: C, 15.0; H, 3.2; N, 8.9; I, 26.5; W, 38.6.

Single crystals suitable for an X-ray structure analysis were grown from a concentrated aqueous solution of the above iodide salt to which a small amount of $Na_2[S_2O_6]$ was added at 80 °C under an argon atmosphere. Very slow cooling of this solution to 20 °C yielded yellow crystals of *syn*-$[L_2W_2O_4]_2(S_2O_6)I_2 \cdot 2H_2O$.

Table I. Summary of Crystallographic Data

	$[C_{12}H_{30}N_6O_4W_2]I_2$	$[C_{12}H_{30}N_6O_4W_2]_2(S_2O_6)I_2 \cdot 2H_2O$
fw	943.9	1680.2
cryst system	monoclinic	orthorhombic
space group	$P2_1/c$	*Pnnm* (No. 58)
Z	2	2
a, Å	6.838 (2)	12.974 (2)
b, Å	11.539 (3)	22.370 (5)
c, Å	14.716 (4)	8.612 (2)
β, deg	90.57 (2)	
vol, Å^3	1161.3 (5)	2499.5 (6)
d_{calcd}, g cm^{-3}	2.698	2.232
cryst dimens, mm	0.18 × 0.20 × 0.65	0.35 × 0.45 × 0.65
temp, °C	25 (1)	25 (1)
diffractometer	Nicolet R3m/V	Nicolet R3m/V
radiation (mono)	Mo Kα (graphite)	Mo Kα (graphite)
scan type	ω–2ϑ	ω–2ϑ
2ϑ range, deg	$3 \ll 2\vartheta \ll 50$	$2 \ll 2\vartheta \ll 45$
data collected	$\pm h,+k,+l$	$+h,\pm k,+l$
no. of data collected	2257	4675
no. of unique data $4\sigma(F)$	1886	1611
no. of parameters	119	152
abs coeff, cm^{-1}	127.5	72.9
abs cor	empirical, ψ scans	empirical, ψ scans
R	0.045	0.064
R_w	0.051	0.059
goodness of fit	2.47	1.98

Preparation of *anti*-$[L_2W_2O_4]I_2$. To a solution of $[L_2W_2O_5](Br_3)_2$[11] (0.7 g) in water (20 mL) was added methanesulfonic acid (4 mL). To the degassed solution was added zinc dust (1.0 g) under an argon atmosphere at room temperature. After 1 h of stirring, NaI (3.0 g) was added to the then clear green solution, initiating the precipitation of a green solid, which was filtered off, washed with ethanol and ether, and dried under argon. This material was redissolved in water (10 mL) in the presence of air and stirred at room temperature in an open vessel.

The pH of the solution was maintained at 7 by addition of $NaHCO_3$ in small amounts. Within $^1/_2$ h the color of the solution changed to purple. Precipitation of purple microcrystals of *anti*-$[L_2W_2O_4]I_2$ was initiated by addition of NaI (2.0 g); yield 0.3 g.

Anal. Calcd for $[(C_6H_{15}N_3)_2W_2O_4]I_2$: C, 15.27; H, 3.20; N, 8.90; I, 26.89; W, 38.95. Found: C, 14.9; H, 3.2; N, 8.7; I, 27.4; W, 39.1.

Single crystals suitable for an X-ray structure analysis were grown from an aqueous solution of the above iodide salt by slowly cooling an at 50 °C saturated solution to 10 °C.

X-ray Structural Determinations. A purple crystal of *anti*-$[L_2W_2O_4]I_2$ (**1**) or a yellow one of *syn*-$[L_2W_2O_4]_2(S_2O_6)I_2 \cdot 2H_2O$ (**2**) was attached to a glass fiber and mounted on a Nicolet R3m/V diffractometer. The respective unit cell dimensions were obtained by a least-squares fit of 28 reflections ($16 \leq 2\vartheta \leq 28°$) for **1** and 40 reflections for **2** ($15 \leq 2\vartheta \leq 30°$): The data are summarized in Table I. Intensity data were corrected for Lorentz and polarization effects; empirical absorption cor-

(1) (a) Ruhr-Universität Bochum. (b) Universität Gesamthochschule Paderborn.
(2) Dori, Z. *Prog. Inorg. Chem.* **1981**, *28*, 239.
(3) Khalil, S.; Sheldrick, B. *Acta Crystallogr., Sect B: Struct. Crystallogr. Cryst. Chem.* **1978**, *B34*, 3751.
(4) Mattes, R.; Mennemann, K. *Z. Anorg. Allg. Chem.* **1977**, *437*, 175.
(5) In $Cl_2O(Ph_3PO)W(\mu\text{-S-}i\text{-Bu})_2W(Ph_3PO)Cl_2O$ the $\{OW(\mu\text{-S-}i\text{-Bu})_2WO\}$ core possesses an anti configuration: Ball, J. M.; Boorman, P. M.; Richardson, J. F. *Inorg. Chem.* **1986**, *25*, 3325.
(6) Stiefel, E. I. *Prog. Inorg. Chem.* **1977**, *22*, 1.
(7) Wieghardt, K.; Hahn, M.; Swiridoff, W.; Weiss, J. *Angew. Chem.* **1983**, *95*, 499; Angew. *Chem., Int. Ed. Engl.* **1983**, *22*, 491.
(8) Wieghardt, K.; Guttmann, M.; Chaudhuri, P.; Gebert, W.; Minelli, M.; Young, C.; Enemark, J. H. *Inorg. Chem.* **1985**, *24*, 3151.
(9) Chaudhuri, P.; Wieghardt, K.; Gebert, W.; Jibril, I.; Huttner, G. *Z. Anorg. Allg. Chem.* **1985**, *521*, 23.
(10) Roy, P. S.; Wieghardt, K. *Inorg. Chem.* **1987**, *26*, 1885.
(11) Chaudhuri, P.; Wieghardt, K.; Tsay, Y. H.; Krüger, C. *Inorg. Chem.* **1984**, *23*, 427.

0020-1669/88/1327-2111$01.50/0

Table II. Atom Coordinates (×10⁴) and Equivalent Isotropic Displacement Parameters (Å² × 10³) of *anti*-$[L_2W_2O_4]I_2$

	x	y	z	U(eq)[a]
W(1)	9291 (1)	910 (1)	5376 (1)	20 (1)
I(1)	3571 (2)	−594 (1)	1603 (1)	35 (1)
O(1)	6772 (17)	825 (10)	5396 (8)	34 (4)
O(2)	9813 (19)	595 (9)	4087 (7)	33 (4)
N(1)	9593 (16)	1709 (13)	6747 (9)	34 (4)
N(2)	9189 (19)	2788 (11)	5080 (9)	27 (4)
N(3)	12531 (17)	1538 (12)	5501 (8)	24 (4)
C(1)	12739 (26)	2463 (16)	4796 (11)	35 (5)
C(2)	13084 (23)	1945 (15)	6434 (11)	30 (5)
C(3)	11162 (28)	3363 (15)	4888 (13)	40 (6)
C(4)	8104 (27)	3359 (16)	5832 (12)	39 (6)
C(5)	11574 (28)	1506 (17)	7111 (11)	40 (6)
C(6)	9065 (30)	3014 (14)	6746 (12)	40 (6)

[a] Equivalent isotropic U defined as one-third of the trace of the orthogonalized U_{ij} tensor.

Table III. Bond Lengths (Å) and Angles (deg) of *anti*-$[L_2W_2O_4]I_2$

W(1)–W(1)	2.568 (1)	W(1)–O(1)	1.726 (11)
W(1)–O(2)	1.968 (11)	W(1)–O(2)	2.001 (11)
W(1)–N(1)	2.226 (13)	W(1)–N(2)	2.212 (13)
W(1)–N(3)	2.337 (12)	N(1)–C(5)	1.470 (21)
N(1)–C(6)	1.549 (21)	N(2)–C(3)	1.533 (20)
N(2)–C(4)	1.491 (21)	N(3)–C(1)	1.496 (20)
N(3)–C(2)	1.496 (20)	C(1)–C(3)	1.504 (27)
C(2)–C(5)	1.528 (24)	C(4)–C(6)	1.544 (26)
W(1)–W(1)–O(1)	110.0 (4)	O(2A)–W(1)–O(1)	101.4 (5)
O(2)–W(1)–O(1)	104.2 (5)	N(1)–W(1)–O(1)	95.3 (5)
N(1)–W(1)–O(2)	159.1 (5)	N(2)–W(1)–O(1)	91.7 (5)
N(2)–W(1)–O(2)	89.8 (5)	N(2)–W(1)–N(1)	77.0 (5)
N(3)–W(1)–O(1)	164.2 (5)	N(3)–W(1)–O(2)	87.3 (5)
N(3)–W(1)–N(1)	73.8 (4)	N(3)–W(1)–N(2)	74.9 (5)
W(1)–O(2)–W(1)	80.6 (4)	C(5)–N(1)–W(1)	109.9 (10)
C(6)–N(1)–W(1)	112.5 (10)	C(6)–N(1)–C(5)	111.7 (13)
C(3)–N(2)–W(1)	115.8 (10)	C(4)–N(2)–W(1)	107.6 (10)
C(4)–N(2)–C(3)	113.0 (13)	C(1)–N(3)–W(1)	105.3 (9)
C(2)–N(3)–W(1)	113.6 (9)	C(2)–N(3)–C(1)	112.8 (13)
C(3)–C(1)–N(3)	110.9 (13)	C(5)–C(2)–N(3)	109.2 (13)
C(1)–C(3)–N(2)	110.5 (13)	C(6)–C(4)–N(2)	108.8 (14)
C(2)–C(5)–N(1)	109.6 (13)	C(4)–C(6)–N(1)	110.4 (13)
O(2)–W(1)–O(2A)	99.4 (4)		

rections (ψ scans) were also carried out for both data sets. The function minimized during least-squares refinements was $\sum w(||F_o| - |F_c||)^2$ with final convergence to $R = \sum||F_o| - |F_c||/\sum|F_o|$, where $w = 1/\sigma^2(F)$. The structures were solved via conventional Patterson and Fourier syntheses. The positions of methylene protons were calculated (d(C–H) = 0.96 Å, sp^3 hybridization at C) and were included in the final refinement cycle with an isotropic temperature factor U = 0.093 Å². All non-hydrogen atoms were refined with use of anisotropic thermal parameters (supplementary material). In the final refinement cycle of the structure of **1** maximum Δ/σ = 0.001 and maximum height in the final ΔF map was 1.3 e/Å³ near the W(1) position; for **2** $(\Delta/\sigma)_{max}$ = 0.001 and maximum height in the final ΔF map was 1.5 e/Å³ near the heavy atom tungsten position. During all calculations the analytical scattering factors for neutral atoms were corrected for both $\Delta f'$ and $i(\Delta f'')$ terms.[12] The final atomic parameters for **1** and **2** are given in Tables II and IV, respectively; bond lengths and selected angles are given in Table III for **1** and Table V for **2**.

Kinetic Measurements. The H^+-catalyzed isomerization reaction *anti*-$[L_2W_2O_4]^{2+} \rightarrow$ *syn*-$[L_2W_2O_4]^{2+}$ was run in acidic aqueous solution ($HClO_4$) under pseudo-first-order conditions (excess $[H^+]$) under an argon atmosphere. The ionic strength was adjusted to 1.0 M with $NaCH_3SO_3$. The decrease of absorption of acidic solutions containing *anti*-$[L_2W_2O_4]I_2$ was monitored at λ = 520 nm (on a UNICAM SP1700 spectrophotometer) as a function of time.

Pseudo-first-order rate constants were calculated by using a least-squares program[13] where the absorption at the beginning of the reaction and after the completed reaction were treated as variables. The observed and calculated values differed only within the uncertainty of the last digit of the readings of the instrument.

(12) *International Tables for X-ray Crystallography*; Kynoch: Birmingham, England, 1974; Vol. 4. All calculations were carried out by using the SHELXTL-PLUS program package (Nicolet, 1987).
(13) DeTar, D. F. *Comput. Chem.* **1978**, *2*, 99.

Table IV. Atom Coordinates (×10⁴) and Equivalent Isotropic Displacement Parameters (Å² × 10³) of *syn*-$[L_2W_2O_4]_2(S_2O_6)I_2 \cdot 2H_2O$

	x	y	z	U(eq)[a]
W(1)	2011 (1)	3690 (1)	0	43 (1)
W(2)	2358 (1)	2562 (1)	0	46 (1)
I(1)	1333 (1)	1463 (1)	5000	66 (1)
S(1)	5522 (4)	366 (2)	0	51 (2)
O(1)	688 (14)	3714 (6)	0	54 (5)
O(2)	1134 (12)	2265 (6)	0	56 (5)
O(3)	2509 (8)	3149 (4)	1599 (14)	49 (4)
O(4)	6570 (14)	92 (9)	0	63 (6)
O(5)	5274 (9)	687 (5)	1447 (15)	75 (4)
N(1)	2034 (10)	4460 (6)	1624 (18)	56 (5)
N(2)	3703 (11)	4071 (7)	0	42 (5)
C(1)	3011 (14)	4616 (12)	2210 (31)	102 (10)
C(2)	1608 (24)	4987 (9)	836 (24)	69 (10)
C(3)	3916 (19)	4391 (13)	1465 (32)	119 (11)
N(3)	2838 (10)	1848 (7)	1701 (20)	60 (5)
N(4)	4130 (19)	2535 (9)	0	73 (8)
C(4)	3816 (19)	1902 (12)	2360 (25)	94 (9)
C(5)	2586 (23)	1236 (9)	887 (34)	70 (11)
C(6)	4540 (29)	2228 (14)	1428 (50)	71 (19)
O(6)	7734 (31)	1828 (18)	0	177 (16)
O(7)	9702 (32)	1303 (14)	0	153 (11)

[a] Equivalent isotropic U defined as one-third of the trace of the orthogonalized U_{ij} tensor.

Table V. Bond Lengths (Å) and Angles (deg) of *syn*-$[L_2W_2O_4]_2(S_2O_6)I_2 \cdot 2H_2O$

W(1)–W(2)	2.565 (1)	W(1)–O(1)	1.717 (18)
W(1)–O(3)	1.944 (10)	W(1)–N(1)	2.218 (14)
W(1)–N(2)	2.355 (14)	W(2)–O(2)	1.721 (15)
W(2)–O(3)	1.913 (11)	W(2)–N(3)	2.255 (16)
W(2)–N(4)	2.299 (25)	S(1)–O(4)	1.492 (18)
S(1)–O(5)	1.474 (12)	N(1)–C(1)	1.408 (23)
N(1)–C(2)	1.468 (26)	N(2)–C(3)	1.476 (24)
C(1)–C(3)	1.430 (31)	N(3)–C(4)	1.397 (28)
N(3)–C(5)	1.571 (26)	N(4)–C(6)	1.505 (28)
C(4)–C(6)	1.435 (43)		
O(1)–W(1)–W(2)	101.9 (5)	O(3)–W(1)–W(2)	47.8 (3)
O(3)–W(1)–O(1)	110.6 (4)	N(1)–W(1)–W(2)	139.6 (4)
N(1)–W(1)–O(1)	89.4 (5)	N(1)–W(1)–O(3)	91.9 (5)
N(2)–W(1)–W(2)	101.1 (4)	N(2)–W(1)–O(1)	157.0 (6)
N(2)–W(1)–O(3)	85.2 (4)	N(2)–W(1)–N(1)	72.9 (4)
O(2)–W(2)–W(1)	102.5 (5)	O(3)–W(2)–W(1)	48.8 (3)
O(3)–W(2)–O(2)	111.0 (4)	N(3)–W(2)–W(1)	138.2 (4)
N(3)–W(2)–O(2)	88.9 (5)	N(3)–W(2)–O(3)	89.5 (5)
N(4)–W(2)–W(1)	101.6 (5)	N(4)–W(2)–O(2)	155.9 (7)
N(4)–W(2)–O(3)	85.2 (5)	N(4)–W(2)–N(3)	72.9 (5)
O(5)–S(1)–O(4)	113.5 (6)	W(2)–O(3)–W(1)	83.4 (5)
C(1)–N(1)–W(1)	115.5 (11)	C(2)–N(1)–W(1)	109.1 (12)
C(2)–N(1)–C(1)	107.8 (19)	C(3)–N(2)–W(1)	110.5 (12)
C(3)–C(1)–N(1)	119.4 (16)	C(1)–C(3)–N(2)	113.6 (17)
C(4)–N(3)–W(2)	116.9 (14)	C(5)–N(3)–W(2)	105.6 (13)
C(5)–N(3)–C(4)	116.5 (17)	C(6)–N(4)–W(2)	111.4 (19)
C(6)–C(4)–N(3)	114.4 (21)	C(4)–C(6)–N(4)	117.2 (25)
C(6)–N(4)–C(6)	109.6 (43)	O(3)–W(1)–O(3A)	90.2 (4)
O(3)–W(2)–O(3A)	92.1 (4)		

Results and Discussion

Syntheses. In a recent publication[9] we have shown that it is possible to generate dimeric *syn*-$[L_2W_2O_4]^{2+}$ by using monomeric $[LWOBr_2]Br$ as starting material. Hydrolysis and dimerization of this complex yielded essentially quantitatively yellow-orange *syn*-$[L_2W_2O_4]I_2$. We have now found a different route to this species. Reduction of monomeric LWO_3[10] or $[L_2W_2O_5](Br_3)_2$[11] dissolved in trifluoromethanesulfonic acid under an argon atmosphere with zinc dust afforded a deep green solution that most probably contained dimeric hydroxo-bridged dimers of tungsten(III) (see below). Exposure of this solution to oxygen (air), after filtering unreacted zinc off, gave an orange-yellow solution, from which solid *syn*-$[L_2W_2O_4]I_2$ precipitated after addition of

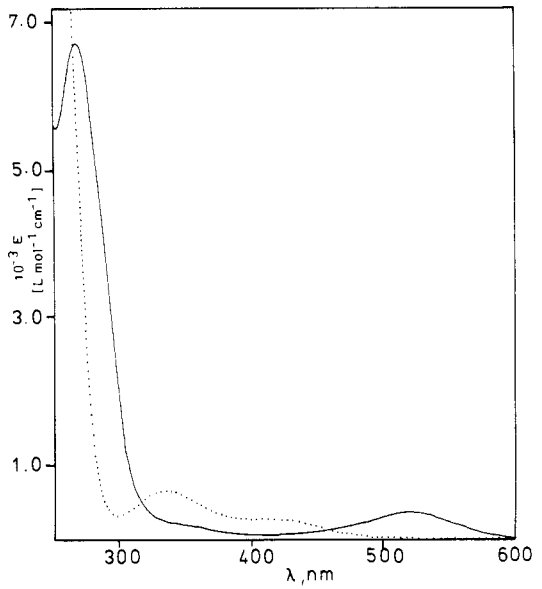

Figure 1. Electronic spectra of *anti*-$[L_2W_2O_4]I_2$ (—) and *syn*-$[L_2W_2O_4]I_2$ (···) in H_2O at 20 °C.

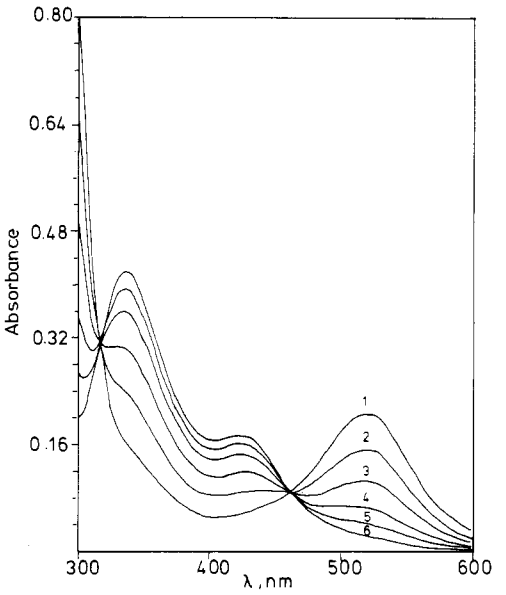

Figure 2. Scan spectrum of the anti → syn isomerization in 1.0 M $HClO_4$ ([anti isomer] = 6.8×10^{-4} M): (1) 0 min; (2) 7 min; (3) 17 min; (4) 31 min; (5) 46 min; (6) 77 min.

solid sodium iodide. In the infrared spectrum (KBr disk) bands at 958 and 728 cm^{-1} are assigned $\nu(W{=}O_t)$ and $\nu_{as}(W{-}O{-}W)$ stretching frequencies. The electronic spectrum exhibits two intense bands in the visible region at 423 nm (ϵ = 335 L mol^{-1} cm^{-1}) and 337 (815), in good agreement with previously published data (Figure 1).[9] The material is diamagnetic.

From an aqueous solution of the iodide salt yellow-orange single crystals of *syn*-$[L_2W_2O_4]_2(S_2O_6)I_2{\cdot}2H_2O$ suitable for an X-ray analysis slowly grew after solid $Na_2S_2O_6$ was added.

If, on the other hand, solid sodium iodide was added to the above green solution under strictly oxygen-free conditions, a green solid[14] precipitated. Redissolving this material in water in the presence of air and maintaining the pH of the solution at 7 by adding small amounts of $NaHCO_3$ yielded a purple solution. After addition of solid sodium iodide purple crystals of *anti*-$[L_2W_2O_4]I_2$ precipitated. In the infrared spectrum (KBr disk) a $\nu(W{=}O_t)$ stretching frequency is observed at 915 cm^{-1}; at 718 cm^{-1} the $\nu_{as}(W{-}O{-}W)$ mode is observed. These data are not in agreement with those published previously for an alleged *anti*-$[L_2W_2O_4]^{2+}$ species.[9] The electronic spectrum of the above material exhibits two bands at 520 nm (ϵ = 360 L mol^{-1} cm^{-1}) and 271 (6.6×10^3). These data also do not agree with the previously published data. Since the above material has now been characterized by X-ray crystallography (see below) to consist of *anti*-$[L_2W_2O_4]^{2+}$ cations and uncoordinated iodide anions, it is not clear to us what the structure of the alleged "brick-red $[L_2W_2O_4]I_2$" in ref 9 is. We are at present trying to grow single crystals suitable for an X-ray analysis of this latter material.

It is noted that the infrared data and the electronic spectra of *syn*- and *anti*-$[L_2W_2O_4]^{2+}$ are strikingly similar to those of their molybdenum analogues.[7,8,15]

anti-$[L_2W_2O_4]^{2+}$ was found to be unstable in acidic aqueous solution; isomerization to the *syn*-$[L_2W_2O_4]^{2+}$ form is observed. In alkaline solution decomposition to an unidentified product was observed, not the anti → syn isomerization as has been described for *anti*-$[L_2Mo_2O_4]^{2+}$.[8,15]

Kinetics and Mechanism of the Anti → Syn Isomerization. Aqueous solutions of *anti*-$[L_2W_2O_4]^{2+}$ in the absence of oxygen are stable at 25 °C for at least 4 days. However, in acidic solutions *anti*-$[L_2W_2O_4]^{2+}$ changes color from purple to yellow. The final spectrum is identical with that of a genuine solution of *syn*-$[L_2W_2O_4]^{2+}$. Repetitive scanning of the spectrum during the reaction reveals two isosbestic points at 318 and 461 nm (Figure 2). The kinetics of this isomerization reaction were followed at 520 nm, the absorption maximum of *anti*-$[L_2W_2O_4]^{2+}$, with $[H^+]$ in large excess (pseudo-first-order conditions). Plots of absorbance changes, log $(A_t - A_\infty)$, against time, t, were linear to at least 5 half-lives of the reaction. Observed first-order rate constants at 25 °C (I = 1.0 M) are given in Table VI. A plot of k_{obsd}^{-1}, s, vs. $[H^+]^{-1}$ is linear as in eq 1, and numerical values for k_a and K_a are 7.25×10^{-3} s^{-1} and 7.8 M.

Table VI. Pseudo-First-Order Rate Constants for the H^+-Catalyzed Anti → Syn Isomerization of *anti*-$[L_2W_2O_4]^{2+}$ [a]

$[H^+]$, M	$10^4 k_{obsd}$, s^{-1}	$[H^+]$, M	$10^4 k_{obsd}$, s^{-1}
0.1	0.92	0.7	6.01
0.4	3.64	1.0	7.88

[a] 25 °C, I = 1.0 M ($NaCH_3SO_3$), $[W^V_2]$ = 3×10^{-4} M.

$$k_{obsd}^{-1} = k_a^{-1} + (K_a/k_a)[H^+] \quad (1)$$

The same rate law has been found for the acid-catalyzed anti → syn isomerization of *anti*-$[L_2Mo_2O_4]^{2+}$,[15] where a mechanism had been proposed that invokes a protonated form of the anti isomer which isomerizes in the rate-determining step (k_a). The same mechanism is proposed to be operative in the present case (eq 2–4). Interestingly, the dissociation constants, K_a, for the

$$anti\text{-}[L_2W_2O_4]^{2+} + H^+ \overset{K_a^{-1}}{\rightleftharpoons} anti\text{-}[L_2W_2O_4H]^{3+} \quad (2)$$

$$anti\text{-}[L_2W_2O_4H]^{3+} \xrightarrow{k_a} syn\text{-}[L_2W_2O_4H]^{3+} \quad (3)$$

$$syn\text{-}[L_2W_2O_4H]^{3+} \xrightarrow{\text{fast}} syn\text{-}[L_2W_2O_4]^{2+} + H^+ \quad (4)$$

molybdenum (2.6 M) and tungsten (7.8 M) anti isomers are quite similar at 25 °C (I = 1.0 M), but the values for the isomerization constant, k_a (s^{-1}), differ significantly. For *anti*-$[L_2Mo_2O_4]^{2+}$ k_a is 4.4×10^{-4} s^{-1} whereas for *anti*-$[L_2W_2O_4]^{2+}$ the isomerization is faster by 1 order of magnitude (k_a = 7.25×10^{-3} s^{-1}).

The actual point of protonation is not known, but the terminal oxo groups are probably more basic than the oxo bridges. Protonation of a W=O group leads to a weakening of this bond, and nucleophilic attack of an H_2O molecule in trans position to the W=OH group is conceivable. Further protonation of this group yields a coordinated H_2O whereas concomitant deprotonation of the incoming H_2O yields a new W=O group in syn position with respect to the other W=O group in the dimer. Now the new water ligand dissociates and the syn isomer is formed (Scheme I).

Crystal Structures of *anti*-$[L_2W_2O_4]I_2$ and *syn*-$[L_2W_2O_4]_2(S_2O_6)I_2{\cdot}2H_2O$. Purple crystals of *anti*-$[L_2W_2O_4]I_2$ consist of the

(14) We are presently investigating the nature of this material. Presumably $[L_2W^{III}_2(\mu\text{-}OH)_2Br_2]I_2$ is formed.[9]

(15) Hahn, M.; Wieghardt, K. *Inorg. Chem.* **1984**, *23*, 3977.

Scheme I

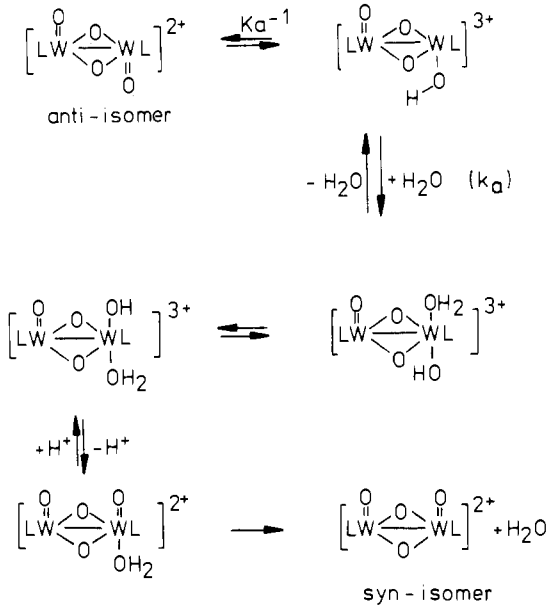

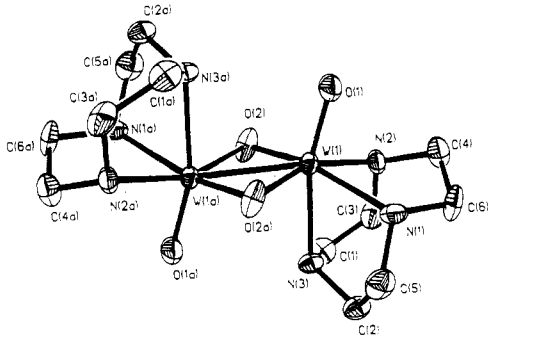

Figure 3. Perspective view and atom-labeling scheme of *anti*-$[L_2W_2O_4]^{2+}$.

dimeric cation *anti*-$[L_2W_2O_4]^{2+}$ and iodide anions. Figure 3 shows the atom-labeling scheme and a perspective view of the cation. Table III summarizes bond distances and angles. The complex cation lies on a crystallographic center of symmetry. Each tungsten atom is in a pseudooctahedral environment comprising three facially coordinated amine nitrogen atoms of the ligand 1,4,7-triazacyclononane and three oxygen atoms, one of which is a terminal oxo group and two of which are bridging W–O–W groups (edge-sharing bioctahedra). The two terminal oxo groups are in anti position with respect to each other, and the W–W distance of 2.568 (1) Å is quite short. The W_2O_2 four-membered ring is planar; the W–O–W bond angles are acute (Chart I) wheras the O–W–O bond angles are obtuse. This, together with the observed diamagnetism of *anti*-$[L_2W_2O_4]^{2+}$, is indicative of a W–W bond of the order 1. The W=O group exerts a strong trans influence since the W–N distance trans to this group is longer by 0.12 Å than the two corresponding W–N distances, which are in trans positions with respect to W–O units. The structure of *anti*-$[L_2W_2O_4]^{2+}$ is virtually identical with that of *anti*-$[L_2Mo_2O_4]^{2+}$ described in ref 7.

Crystals of *syn*-$[L_2W_2O_4]_2(S_2O_6)I_2 \cdot 2H_2O$ consist of the dimeric cation *syn*-$[L_2W_2O_4]^{2+}$, dithionate and iodide anions, and water molecules of crystallization. Figure 4 shows the cation and the atom-labeling scheme; Table V summarizes bond distances and angles. Each tungsten atom is again in a pseudooctahedral environment of the amine ligand, terminal oxo groups, and two bridging oxygen atoms; but, in contrast to the case of *anti*-$[L_2W_2O_4]^{2+}$, the two terminal oxo groups are now in syn position with respect to each other. The W—N and W=O_t bond distances are within experimental error identical with the corresponding bond lengths in *anti*-$[L_2W_2O_4]^{2+}$, but the W—O_b distances are

Chart I

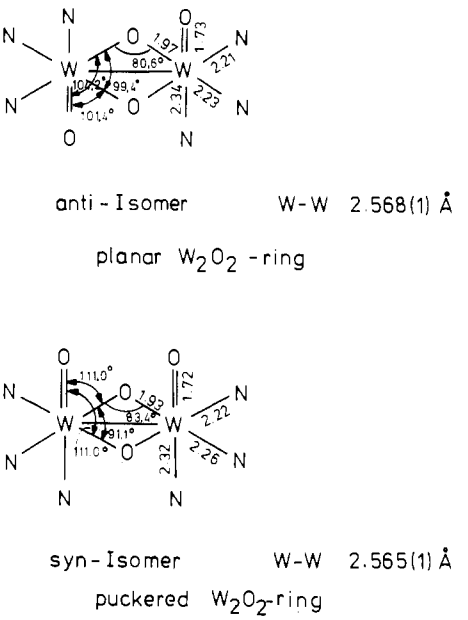

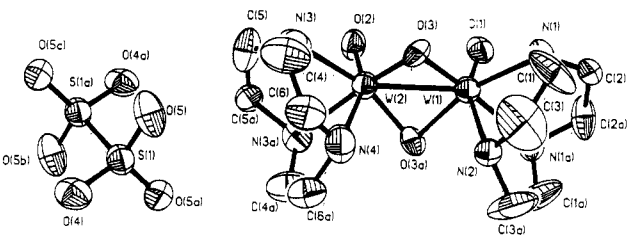

Figure 4. Perspective view and atom-labeling scheme of the *syn*-$[L_2W_2O_4]_2(S_2O_6)I_2 \cdot 2H_2O$.

different (Chart I). Contrasting the planar W_2O_2 four-membered ring in *anti*-$[L_2W_2O_4]^{2+}$, this ring is puckered in *syn*-$[L_2W_2O_4]^{2+}$, as is the case in other complexes containing the *syn*-$\{W_2O_4\}^{2+}$ core. The W—W distance is 2.565 (1) Å, which is identical with the one in *anti*-$[L_2W_2O_4]^{2+}$ and is also indicative of a metal–metal bond of the order 1.

The question as to why the syn isomer is thermodynamically more stable than the anti isomer may be analyzed by following closely the discussion for *anti*- and *syn*-$[L_2Mo_2O_4]^{2+}$ presented recently in ref 8 and 15. It is instructive to compare the sum of the three bond angles O–W–O in both structures. For the anti isomer this sum is calculated to be 305° whereas for the syn isomer a value of 314° is found. The nonbonding overall distance between the oxygen atoms of the LWO_3 moieties of the syn isomer $\sum_1^3 d(O\cdots O)$ is 8.78 compared to 8.83 Å in the anti isomer; they are identical within experimental error. This is in contrast to the isomers of $[L_2Mo_2O_4]^{2+}$, where the syn isomer exhibits an increased overall nonbonding O···O distance compared to the anti isomer. The terminal W=O_t bonds are the same in both structures, but the W—O_b bond lengths are significantly different, being longer in the anti isomer (average 1.98 (1) Å) than in the syn isomer (1.93 (1) Å). Thus there is no straightforward structural interpretation for the stability of the syn isomer detected.

Theoretical calculations on the *syn*- and *anti*-$[Mo_2S_4(S_2C_2H_4)_2]^{2-}$ ions have shown that the direct Mo—Mo bonding interaction is more stable in the syn isomer.[16] A direct π-bonding interaction between the two Mo=O units in *syn*-$[Mo_2O_2S_2(S_2)_2]^{2-}$ has also been proposed,[17] which is not possible in the anti isomer. Steric interactions among coordinated ligands[18,19] as well as inter-

(16) Chandler, T.; Lichtenberger, D. L.; Enemark, J. H. *Inorg. Chem.* **1981**, *20*, 75.
(17) Bernholc, J.; Holzwarth, N. A. W. *J. Chem. Phys.* **1984**, *81*, 3987.
(18) Gelder, J.; Enemark, J. H. *Inorg. Chem.* **1976**, *15*, 1839.
(19) Newsam, J.; Halbert, T. *Inorg. Chem.* **1985**, *24*, 491.

and intramolecular hydrogen bonding involving the terminal oxo groups and the NH groups of the ligand[20] may also contribute, although in the present case this seems not to be the case since no such interactions are detectable in *syn*- or *anti*-$[L_2W_2O_4]^{2+}$.

Acknowledgment. We thank the Fonds der Chemischen Industrie for financial support. Dr. P. Chaudhuri (Bochum) is thanked for helpful suggestions concerning the preparation of complexes.

Registry No. 1, 97414-60-3; 2, 114376-24-8; *syn*-$[L_2W_2O_4]I_2$, 97373-51-8; LWO_3, 108344-95-2; $[L_2W_2O_5](Br_3)_2$, 114299-76-2; Zn, 7440-66-6.

Supplementary Material Available: Tables S1-S4, listing anisotropic thermal parameters and calculated positions of hydrogen atoms (2 pages); tables of calculated and observed structure factors for *anti*-$[L_2W_2O_4]I_2$ and *syn*-$[L_2W_2O_4]_2(S_2O_6)I_2 \cdot 2H_2O$ (13 pages). Ordering information is given on any current masthead page.

(20) Marabella, C. P.; Enemark, J. H.; Müller, K. F.; Bruce, A.; Pariyadath, N.; Corbin, J. L.; Stiefel, E. I. *Inorg. Chem.* **1983**, *22*, 3456.

Contribution from the Institut für Anorganische Chemie, Universität Bern, CH-3000 Bern 9, Switzerland, Solid State Department, Rijksuniversiteit Utrecht, NL-3508 TA Utrecht, The Netherlands, and Lehrstuhl für Anorganische Chemie I, Ruhr Universität, D-4630 Bochum 1, Federal Republic of Germany

Optical Absorption and Luminescence Spectroscopy of $[LCr(OH)(CH_3COO)_2CrL](ClO_4)_3$ and $[LCr(OH)(CH_3COO)_2ZnL](ClO_4)_2 \cdot 0.5H_2O$ (L = 1,4,7-Trimethyl-1,4,7-triazacyclononane)

Christian Reber,[1a] Hans U. Güdel,*[1a] Maarten Buijs,[1b] Karl Wieghardt,[1c] and Phalguni Chaudhuri[1c]

Received November 6, 1987

The optical spectroscopic properties of the title compounds were investigated by single-crystal absorption and luminescence spectroscopy as well as luminescence decay measurements between 1.8 K and room temperature. With a luminescence line-narrowing technique, accurate values for the ground-state exchange parameters were determined for $[LCr(OH)(CH_3COO)_2CrL](ClO_4)_3$, with L = 1,4,7-trimethyl-1,4,7-triazacyclononane: $J = -14.6$ cm^{-1} and $j = 0.1$ cm^{-1} with $\hat{H}_{ex} = -2J(\vec{S}_1 \cdot \vec{S}_2) - j(\vec{S}_1 \cdot \vec{S}_2)^2$. The emitting state is shown to have $S = 1$. In $[LCr(OH)(CH_3COO)_2ZnL](ClO_4)_2 \cdot 0.5H_2O$ the presence of nonradiative transfer of excitation energy between crystallographically inequivalent dinuclear units is established. A simple kinetic model is able to quantitatively account for the observed luminescence decay behavior.

1. Introduction

The optical spectroscopic properties of chromium(III) compounds have continuously been the subject of intensive study for more than 2 decades.[2,3] The main interest among coordination chemists is in the understanding of the photochemical properties of chromium (III) complexes.[4] In the solid-state sciences one of the main emphases is on chromium(III)-doped crystals and glasses as possible candidates for new laser materials.[5] Understanding the relaxation and energy-transfer processes is very important for designing new solids suitable for application as lasers. The study of exchange-coupled chromium(III) pairs, which has been an active area of research for some time, has both chemically and physically relevant aspects.[6,7] Besides the synthesis of new compounds, one of the main aims has been the establishment of correlations between various physical properties and the structure.[8]

The tridentate chelate ligand L = 1,4,7-trimethyl-1,4,7-triazacyclononane has opened the way to a new family of dinuclear complexes. $[LCr(OH)_3CrL]^{3+}$ was the first trihydroxo-bridged chromium(III) complex to be synthesized.[9] Variation of the metal ions in this dinuclear unit is possible, and both homonuclear and heteronuclear complexes have been prepared.[10] Another possibility is the variation of the bridging ligands and the bridging geometry. The title compounds $[LCr(OH)(CH_3COO)_2CrL](ClO_4)_3$ (abbreviated {CrCr}) and $[LCr(OH)(CH_3COO)_2ZnL](ClO_4)_2 \cdot 0.5H_2O$ (abbreviated {CrZn}) have been synthesized very recently.[10] They exhibit a new type of triply bridged dinuclear structure. {CrCr} has been magnetochemically characterized, and a value for the exchange parameter, $J = -15.5$ cm^{-1}, based on the Hamiltonian of eq 1, has been estimated from the temperature dependence of the powder magnetic susceptibility.[10]

The study of exchange interactions in triply bridged chromium(III) pairs is relatively new, and only a few investigations have been reported.[11-13] The optical spectroscopic properties of $[LCr(OH)_3CrL](ClO_4)_3$ have been studied in great detail.[11] High-resolution single-crystal spectroscopy down to 1.5 K turned out to be very informative, and the mechanism of the exchange coupling could be elucidated in detail. In the present study we use spectroscopic techniques, which are well-established in the field of chromium(III)-doped systems but which have only scarcely been applied to pure coordination compounds. The technique of luminescence line narrowing provides a very accurate picture of the first excited state and the exchange splittings in the ground state of {CrCr}. Singly ({CrCr} and {CrZn}) and doubly ({CrCr}) excited states are explored by single-crystal absorption spectroscopy. The comparison of {CrCr} and {CrZn} in the region of ^2E and $^2T_1$ excitations allows an estimate of the various contributions to the observed spectroscopic splittings. {CrZn} is shown to have two crystallographically inequivalent dimer sites. Excitation energy transfer between the sites takes place as a result of weak intermolecular interactions. Time-resolved and site-selective laser spectroscopies provide the necessary data for a quantitative understanding of these phenomena.

The spectroscopic methods used in this study are highly selective. In contrast to bulk techniques, they provide access to the

(1) (a) Universität Bern. (b) Rijksuniversiteit Utrecht. (c) Ruhr Universität.
(2) Ferguson, J. *Prog. Inorg. Chem.* **1970**, *12*, 159.
(3) Imbusch, G. F. In *Luminescence of Inorganic Solids*; Di Bartolo, B., Ed.; Plenum: New York, 1978.
(4) Endicott, J. F.; Ryu, C. K. *Comments Inorg. Chem.* **1987**, *6*, 91.
(5) *Tunable Solid State Lasers*; Hammerling, P., Budgor, A. B., Pinto, A., Eds.; Springer Series in Optical Sciences 47; Springer: West Berlin, 1985.
(6) Güdel, H. U. *Comments Inorg. Chem.* **1984**, *3*, 189.
(7) McCarthy, P. J.; Güdel, H. U., submitted for publication in *Coord. Chem. Rev.*
(8) Hodgson, D. J. In *Magneto-Structural Correlations in Exchange Coupled Systems*; Willett, R. D., Ed.; D. Reidel: Dordrecht, The Netherlands, 1985.
(9) Wieghardt, K.; Chaudhuri, P.; Nuber, B.; Weiss, J. *Inorg. Chem.* **1982**, *21*, 3086.
(10) Chaudhuri, P.; Winter, M.; Küppers, H.-J.; Wieghardt, K.; Nuber, B.; Weiss, J. *Inorg. Chem.* **1987**, *26*, 3302.
(11) Riesen, H.; Güdel, H. U. *Mol. Phys.* **1987**, *60*, 1221.
(12) Bolster, D. E.; Gütlich, P.; Hatfield, W. E.; Kremer, S.; Müller, E. W.; Wieghardt, K. *Inorg. Chem.* **1983**, *22*, 1725.
(13) Riesen, H.; Güdel, H. U. *Chem. Phys. Lett.* **1987**, *133*, 429.

0020-1669/88/1327-2115$01.50/0